Critically ill SARS-CoV-2 patients display lupus-like hallmarks of extrafollicular B cell activation

Authors:

Matthew C. Woodruff[1,4], Richard P. Ramonell[2,4], Kevin S. Cashman[1], Doan C. Nguyen[2], Ariel M. Ley[2], Shuya Kyu[2], Ankur Saini[1], Natalie Haddad[2], Weirong Chen[1], J. Christina Howell[3], Tugba Ozturk[3], Saeyun Lee[2], Jacob Estrada[1], Andrea Morrison-Porter[2], Andrew Derrico[2], Fabliha A. Anam[1], Henry Wu[4], Sang N. Le[1,2], Scott A. Jenks[1], William T. Hu[3], F. Eun-Hyung Lee[2], Ignacio Sanz[1].

Affiliations:

[1]Department of Medicine, Division of Rheumatology, Lowance Center for Human Immunology, Emory University, Atlanta, GA, USA
[2]Department of Medicine, Division of Pulmonary, Allergy, Critical Care and Sleep Medicine, Emory University, Atlanta, GA, USA
[3]Department of Neurology, Emory University, Atlanta, GA
[4]Department of Medicine, Division of Infectious Diseases, Emory University, Atlanta, GA
[5]These authors contributed equally: Matthew C. Woodruff and Richard P. Ramonell

Abstract/Introduction

Wide heterogeneity of disease course ranging from asymptomatic spread [1, 2] to respiratory failure and death [3, 4] has become a hallmark of the SARS-CoV-2 (COVID-19) pandemic. While this clinical spectrum is well documented, its immunologic underpinnings are less clear. We have therefore initiated studies of the B cell responses as they would participate in both early effector responses and in the initiation of memory formation. In terms of effector responses, we were particularly interested in the engagement and clinical correlates of the extra-follicular pathway (EF) we recently described in flaring SLE [5]. In this systemic autoimmune disease, the EF pathway is initiated by newly activated naïve B cell (aN) leading to large expansion of autoantibody-producing antibody-secreting cells through the generation of an epigenetically primed B cell precursor which are double negative (DN) for naïve (IgD) and memory markers (CD27) and lacking expression of CXCR5 and CD21 (DN2) [6, 7, 8]. These highly activated D2 cells are also distinguished by high expression of CD11c and T-bet and are TLR7-driven. Both TLR7-stimulation which is triggered by ssRNA and the central role played by their murine counterparts (typically characterized as Age-Associated B cells), in viral clearance, strongly supported the hypothesis that DN2 cells and the global EF pathway could be prominently engaged in COVID-19 patients [9]. Also of note, EF B cell activation is particularly prominent in SLE patients of African-American ancestry, a population disproportionately represented in severe COVID-19 [6, 9].

In this study we find that critically ill patients with COVID-19 robustly upregulate B cells within the extrafollicular pathway, produce enormous numbers of antibody secreting cells, and lose unique transitional B cell populations that correlate with positive prognosis. This patient cluster associates tightly with biomarkers of poor outcomes and exhibits high rates of mortality. Thus, this B cell phenotype might serve as an immunological marker of severe COVID-19 infection at early stages and could therefore identify a patient subset likely to benefit from targeted immunomodulatory therapy aimed at alleviating disease burden.

Results/Conclusions

As efforts intensify to identify treatment options and develop preventative vaccination strategies against COVID-19 infection [10, 11, 12, 13, 14, 15], there is an urgent need for accurate characterization of protective (and non-protective) humoral responses. With the recent description of a verified human extrafollicular B cell response, the continued identification of new human B cell subsets [16, 17, 18, 19], and the complexity of B cell nomenclature across the literature [20], the development of deep B cell panels capable of accurately identifying B cell subsets while also providing functional context is important in understanding the normal course of SARS-CoV-2 infection. To this end, a high-dimensionality spectral flow cytometry panel targeting human B cells was developed for the following reasons: 1. accurately identifying B cell populations through an extensive set of commonly used lineage markers 2. assessing responsiveness with markers of surface activation, and 3. understanding B cell trafficking through chemokine receptor and selectin expression (Supplemental Table 1).

To characterize humoral B cell response, we enrolled 17 patients with confirmed COVID-19 infection and 22 healthy adults (Supplemental Table 2). Of the COVID-19 group, nine were hospitalized and critically-ill requiring ICU admission with three of the 9 patients who eventually died. Peripheral blood was collected from these patients with a mean collection date of 12 days post-symptom onset to help ensure peak immune characterization.

Despite early reports of lymphocytopenia [21], initial characterizations of COVID-19 infection revealed an expanded CD19+ B cell fraction within the CD45+ hematopoietic compartment in comparison to healthy donors (Fig 1a). Detailed profiling of PBMCs in the COVID-19 cohort focused on the identification of primary populations within total CD19+ B cells (transitional [T], naive [NAV], double negative [DN], memory [M], and antibody secreting cells [ASCs]) (Fig 1b). Subgating these primary populations yielded 15 total non-redundant, secondary B cell populations of established significance in the literature [20] (Fig 1b, Supp Table 3) to be used for multivariate patient clustering. Patients diagnosed with COVID-19 clustered independently from healthy controls, driven primarily by a population cluster containing ASCs and constituents of the extrafollicular (EF) response pathway such as active naive (aN) and double negative 2 (DN2) cells [17] (Fig 1c). Direct assessment

of COVID-19^{+} patient ASCs revealed a significant increase over healthy controls (Fig 1d), and substantial ASC maturation as indicated by high expression of the plasma cell marker CD138 (Fig 1e). Counterintuitively, while ASC generation and maturation are often correlates of protection in vaccine responses [22], in patients with COVID-19 increased ASC instead portended negative disease outcomes with ICU-admitted patients presenting with significantly more ASCs than their HD and outpatient counterparts (Fig 1f).

Closer examination of the initial clustering separated the COVID-19+ patients into two distinct clusters. By removing the healthy donors and re-clustering, two groups of COVID-19 patients resulted with strong upregulation of the EF response pathway (EF-Cov), and those with a muted EF response but enhanced transitional B cell signal (Tr-COV) (Fig 2a). This was not a reflection of infection duration as both clusters were sampled at similar times post symptom onset (Fig 2b). Re-assessment of ASC expansion revealed significantly higher frequencies in the EF-CoV cluster, averaging >10% of CD19+ B cells – well above frequencies after robust vaccine responses that include quadrivalent influenza virus, hepatitis A, tetanus toxoid, and yellow fever vaccines (Fig 2c). Enriched ASC maturation, and increases in the aN and DN2 B cell compartments also correlated with ASC expansion within the EF-CoV cluster, but not in the Tr-CoV cluster or healthy donors (Fig 2d-e). Surprisingly, the composition of the DN compartment, a key indicator of EF response skewing, appeared almost identical to patients with active SLE in the replacement of the switch-memory (sM) associated DN1 population with the ASC-associated DN2 subset (Fig 2f-h).

EF response characterization has identified the pathway as peripherally focused, inflammatory, and highly associated with IL-6 and IP-10 [23, 24]. Indeed, chemokine receptor analysis of EF populations showed a significant decrease in central homing predisposition (CD62L, CXCR5) (Fig 2i). Instead, CXCR3 expression across the subsets, coupled with increased levels of IP-10 within the plasma of the EF-Cov cluster is highly suggestive of peripheral homing to inflamed tissue sites as described in both lung [25] and kidney [26] (Fig 2j-k). Indeed, the two highest cytokine correlates of the EF pathway, IP-10 and IL-6 [23, 24], are strongly upregulated in EF-Cov cluster and reflect the associations with poor outcome prognosis in emerging SARS-CoV-2 literature [27, 28] (Fig 2k-l).

EF pathway enrichment was notable with concomitant decrease of the transitional B cells, particularly a unique $CD21^{lo}$ population making up as much as 10% of the total CD19+ B cells in the Tr-COV2 cluster (Fig 2a, 3a-d). Surprisingly, while these cells shared several of the phenotypic markers of B cell immaturity such as high levels of CD10 and CD38 (Fig 3e), they also expressed high levels of surface IgM with muted surface IgD (Fig 3f), expression of the extrafollicular homing cues (Fig 3g), and an increased expression of the plasma cell marker CD138 (Fig 3h). In SLE, previous studies have identified the direct conversion of transitional B cell populations into ASCs in a polyclonal, autoreactive, and TLR-7 dependent manner [29]. Assessment of our SLE cohort revealed that while transitional populations were frequently decreased in comparison to healthy donors, $CD21^{lo}$ transitional cell proportions were similar to COVID-19^{+} patients (Fig 3i). Yellow Fever vaccinated patients show similar skewing, peaking at d12 post-vaccination (Fig 3j-k). Alongside previous identification in HIV viremia [30], these data suggest that this population may routinely emerge during ssRNA-antiviral responses. Due to their unique phenotype and association with mild disease, it will be important in future studies to fully characterize these cells and understand their impact on the clinical course of infection.

To contextualize differences in clinical trajectory between the EF-CoV and Tr-CoV clusters, longitudinal data was collected from two patients within each cohort. All four were African American, and admitted to the ICU (Fig 4a). While all of the patients displayed ASC expansion, the two from the EF-CoV cohort displayed consistently low levels of transitional B cells (Fig 4b-c). These B cell subset parameters were associated with elevated Sequential Organ Failure Assessment (SOFA) scores (a marker of critical illness severity), and a corresponding decrease in PaO2 to FiO2 ratios – a prognostic measure of gas exchange efficiency while on mechanical ventilation (Fig 4d-e). Additionally, these patients displayed elevated levels of C-reactive protein levels in the blood over their Tr-CoV counterparts (Fig 4f). CRP, an acute phase reactant in the IL-6 pathway, has been increasingly used as a biomarker of COVID-19 severity [31, 32]. This trend in CRP values was generalizable, with blood CRP levels elevated across all critically ill SARS-CoV-2 patients, but particularly those within the IL-6-high EF-CoV cohort (Fig 4g). Surprisingly, linear regression demonstrated that both the low frequency of transitional B cells and a high number of DN2 B cells across patients were correlated as strongly with CRP as IL-6 directly (Fig 4h-j). Finally, as anticipated by their accumulation of poor prognostic

markers, patients within the EF-CoV group faced poor disease outcomes – EF-1 died on day 7 post-symptom onset and EF-2 was still critically ill as of day 24 post-symptom onset. More generally, this cohort suffered an exceptionally high disease burden with (5/6) experiencing kidney failure, 50% mortality and expected to rise. All patients in the Tr-CoV cluster were mild outpatients or have matriculated out of the ICU patient and near discharge.

COVID-19 has vexed clinicians across the globe with its spectrum of illness severity and seemingly maladaptive immune response. Through careful humoral immunophenotyping, the current study offers four important observations in the clinical course in cases of severe illness: 1. while ASCs are robustly expanded in serious infection, their presence cannot be considered a correlate of productive or protective immunity. While the present studies do not address the possible production of anti-COVID-19 antibodies by the expanded ASC, their expansion in early infection carries an ominous prognosis. Whether this just a reflection of an exuberant inflammatory responses or indicates a direct role of ASC in pathogenic responses through the generation of pathogenic antibodies or perhaps pro-inflammatory cytokines, remains to be determined [33, 34]. It is worth noting however, that IL-6 is a major factor in the differentiation of human plasma cells together with Type I IFN [35]; 2. serious SARS-CoV-2 illness is highly associated with the same peripherally targeted and inflammatory extrafollicular response pathways found in serious autoimmune disorders; 3. decrease of transitional B cell pathways, whether correlative or causative, is an important indicator of poor disease outcome. Whether this observation reflects the loss of B cell regulatory function as postulated in SLE and other auto-inflammatory disorders, remains to be elucidated[36]; and 4. due to disease heterogeneity, immunomodulatory therapy such as IL-6 inhibition may have discordant effects on different patient groups. Finally, it will be critical to determine if, as in SLE, pre-disposition towards extrafollicular B-cell activation may be compounding with socio-economic factors to result in the poor infection outcomes observed in the African American population.

Methods

Human Subjects

All research was approved by the Emory University Institutional Review Board (Emory IRB numbers IRB00058507, IRB00057983, and IRB00058271) and was performed in accordance with all relevant guidelines and regulations. Written informed consent was obtained from all participants or, if they were unable to provide informed consent, obtained from designated healthcare surrogates. Healthy donors (n = 22) were recruited using promotional materials approved by the Emory University Institutional Review Board. Subjects with COVID-19 (n = 17) were recruited from Emory University Hospital, Emory University Hospital Midtown and Emory St. Joseph's Hospital, all in Atlanta, GA, USA. All non-healthy donor subjects were diagnosed with COVID-19 by PCR amplification of SARS-CoV-2 viral RNA obtained from nasopharyngeal or oropharyngeal swabs with the exception of one subject, who had serologic evidence of SARS-CoV-2 infection. Subjects with COVID-19 were included in the study if they were 18 to 80 years of age, not immunocompromised, and had not been given oral or intravenous corticosteroids within the preceding 14 days. Peripheral blood was collected in either heparin sodium tubes (PBMCs) (BD Diagnostic Systems) or serum tubes (serum) (BD Diagnostic Systems). Baseline subject demographics are included in Table 2.

To compare ASC responses between COVID-19 infection and vaccine responses, data was used from an additional healthy donors (n = 22) were recruited at Emory University who had not received a vaccination or experienced illness in the past 4 weeks prior to enrollment. Furthermore, 74 adults who received any of the following vaccines were recruited: quadrivalent influenza virus vaccine (n = 28), hepatitis A vaccine (n = 18), tetanus toxoid vaccine (n = 11), and live attenuated yellow fever virus vaccine (n = 17). Peripheral blood was collected in heparin sodium tubes (PBMCs) (BD Diagnostic Systems) at the peak of the ASC responses. Baseline subject demographics are included in Table 3.

Yellow Fever Vaccination

Two subjects after receiving the yellow fever vaccine were enrolled in this study at Emory University in 2019. informed consent was given by all study subjects. PBMCs were isolated on the day the donor received the vaccine and on subsequent days after vaccination as reported in Fig 3.

Peripheral Blood Mononuclear Cell Isolation and Plasma Collection

Peripheral blood samples were collected in heparin sodium tubes and processed within 6 hours of collection. PBMCs were isolated by density gradient centrifugation at 1000 x g for 10 minutes. Aliquots from the plasma layer were collected and stored at -80C until use. PBMCs were washed 2 times with RPMI at 500 x g for 5 minutes. Viability was assessed using trypan blue exclusion and live cells were counted using an automated hemocytometer.

Flow Cytometric Immunophenotyping

Cells were centrifuged again at 500 x g for 5 minutes, the supernatant was removed, and the cells were resuspended in one of two Ab cocktails (below). Cells were stained for 20 minutes at 4C in staining buffer, fixed for 10min in 0.4% PFA, and then washed for immediate flow cytometric immunophenotyping. Cells were analyzed on a Cytek Aurora flow cytometer using Cytek SpectroFlo software. Up to 3 x 106 cells were analyzed using FlowJo v10 (Treestar) software.

Cytokine and Chemokine Multiplex Immunoassay

Plasma levels of several cytokines and chemokines, including IL-1α, IL-1β, IL-2, IL-4, IL-6, IL-7, IL-8, IL-9, IL-10, IL-12, IP-10, TNFα, MDC, MCP-1, and IFNγ were measured using a multiplex immunoassay (Milliplex Human Cytokine/Chemokine Panel, MilliporeSigma, Brulington, MA) in a Luminex-200 platform following manufacturer's protocol (25 mL of neat plasma in duplicates). CRP was measured in a singleplex immunoassay (MilliporeSigma, Burlington, MA) in a Luminex-200 platform following manufacturer's protocol (25 mL of 1:40,000 dilution in duplicates).

Statistical Analysis

Statistical analysis was carried out using Prism statistical analysis software. For each experiment, the type of statistical testing, summary statistics, and levels of significance can be found in the figures and corresponding figure legends

Acknowledgments

We would like to thank all of the healthy volunteers, patients, and their families for their selfless participation in this study. We would also like to thank the nurses, staff, and providers in the 71 ICU in Emory University Hospital Midtown and the 2E ICU in Emory Saint Joseph's Hospital without whom our work could not have been possible. We would like to acknowledge the contributions of Dr. Bashar Staitieh, Dr. David Murphy, Dr. William Bender, Dr. Colin Swenson, Sang Le, Dr. Vanessa Engineer, Mindy Hernandez, and John Varghese for their time and expertise.

Funding

This work was supported by National Institutes of Health grants: R01-AG054991 (W.T.H.), U19-AI110483 Emory Autoimmunity Center of Excellence (I.S.), P01-AI125180-01 (I.S., F.E.L.), R37-AI049660 (I.S.), and T32-HL116271-07 (R.P.R.).

COIs

Dr. Lee is the founder of MicroB-plex, Inc and has research grants with Genentech. Dr. Hu has consulted for ViveBio LLC, AARP Inc, and Biogen Inc; has received research support from Fujirebio US; and has a patent on CSF-based diagnosis of FTLD-TDP.

References

1. Arons, M.M. *et al.* Presymptomatic SARS-CoV-2 Infections and Transmission in a Skilled Nursing Facility. *New England Journal of Medicine* (2020).

2. Wu, C. *et al.* Risk Factors Associated With Acute Respiratory Distress Syndrome and Death in Patients With Coronavirus Disease 2019 Pneumonia in Wuhan, China. *JAMA Internal Medicine* (2020).

3. Guan, W.-j. *et al.* Clinical characteristics of coronavirus disease 2019 in China. *New England Journal of Medicine* (2020).

4. Zhou, F. *et al.* Clinical course and risk factors for mortality of adult inpatients with COVID-19 in Wuhan, China: a retrospective cohort study. *The Lancet* (2020).

5. Jenks, S.A., Cashman, K.S., Woodruff, M.C., Lee, F.E.-H. & Sanz, I. Extrafollicular responses in humans and SLE. *Immunological Reviews* **288**, 136-148 (2019).

6. Jenks, S.A. *et al.* Distinct Effector B Cells Induced by Unregulated Toll-like Receptor 7 Contribute to Pathogenic Responses in Systemic Lupus Erythematosus. *Immunity* **49**, 725-739.e726 (2018).

7. Tipton, C.M. *et al.* Diversity, cellular origin and autoreactivity of antibody-secreting cell population expansions in acute systemic lupus erythematosus. *Nature immunology* **16**, 755-765 (2015).

8. Scharer, C.D. *et al.* Epigenetic programming underpins B cell dysfunction in human SLE. *Nature immunology* **https://doi.org/10.1038/s41590-019-0419-9** (2019).

9. Rubtsova, K., Rubtsov, A.V., Cancro, M.P. & Marrack, P. Age-Associated B Cells: A T-bet-Dependent Effector with Roles in Protective and Pathogenic Immunity. *Journal of immunology (Baltimore, Md. : 1950)* **195**, 1933-1937 (2015).

10. Xu, X. *et al.* Effective treatment of severe COVID-19 patients with tocilizumab. *ChinaXiv* **202003**, v1 (2020).

11. Shen, C. *et al.* Treatment of 5 critically ill patients with COVID-19 with convalescent plasma. *Jama* (2020).

12. Stebbing, J. *et al.* COVID-19: combining antiviral and anti-inflammatory treatments. *The Lancet Infectious Diseases* **20**, 400-402 (2020).

13. Park, T. *et al.* Spike protein binding prediction with neutralizing antibodies of SARS-CoV-2. *bioRxiv*, 2020.2002.2022.951178 (2020).

14. Crosby, J.C. *et al.* COVID-19: A Review of Therapeutics Under Investigation. *Journal of the American College of Emergency Physicians Open* (2020).

15. Michot, J.-M. *et al.* Tocilizumab, an anti-IL6 receptor antibody, to treat COVID-19-related respiratory failure: a case report. *Annals of Oncology* (2020).

16. Warsame, A. *et al.* Monocytoid B cells: an enigmatic B cell subset showing evidence of extrafollicular immunoglobulin gene somatic hypermutation. *Scandinavian journal of immunology* **75**, 500-509 (2012).

17. Jenks, S.A. *et al.* Distinct effector B cells induced by unregulated toll-like receptor 7 contribute to pathogenic responses in systemic lupus erythematosus. *Immunity* **49**, 725-739. e726 (2018).

18. Wang, S. *et al.* IL-21 drives expansion and plasma cell differentiation of autoreactive CD11c(hi)T-bet(+) B cells in SLE. *Nat Commun* **9**, 1758 (2018).

19. Jenks, S.A., Cashman, K.S., Woodruff, M.C., Lee, F.E.H. & Sanz, I. Extrafollicular responses in humans and SLE. *Immunological reviews* **288**, 136-148 (2019).

20. Sanz, I. *et al.* Challenges and Opportunities for Consistent Classification of Human B Cell and Plasma Cell Populations. *Frontiers in immunology* **10**, 2458 (2019).

21. Tan, L. *et al.* Lymphopenia predicts disease severity of COVID-19: a descriptive and predictive study. *Signal transduction and targeted therapy* **5**, 1-3 (2020).

22. Henn, A.D. *et al.* High-resolution temporal response patterns to influenza vaccine reveal a distinct human plasma cell gene signature. *Scientific reports* **3**, 2327 (2013).

23. Xu, W. *et al.* Macrophages induce differentiation of plasma cells through CXCL10/IP-10. *Journal of Experimental Medicine* **209**, 1813-1823 (2012).

24. Sebina, I. *et al.* IL-6 promotes CD4+ T-cell and B-cell activation during Plasmodium infection. *Parasite immunology* **39**, e12455 (2017).

25. Onodera, T. *et al.* Memory B cells in the lung participate in protective humoral immune responses to pulmonary influenza virus reinfection. *Proceedings of the National Academy of Sciences* **109**, 2485-2490 (2012).

26. Lacotte, S. *et al.* Early differentiated CD138highMHCII+ IgG+ plasma cells express CXCR3 and localize into inflamed kidneys of lupus mice. *PloS one* **8** (2013).

27. Chen, X. *et al.* Detectable serum SARS-CoV-2 viral load (RNAaemia) is closely associated with drastically elevated interleukin 6 (IL-6) level in critically ill COVID-19 patients. *medRxiv* (2020).

28. Yang, Y. *et al.* Exuberant elevation of IP-10, MCP-3 and IL-1ra during SARS-CoV-2 infection is associated with disease severity and fatal outcome. *medRxiv* (2020).

29. Wang, T. *et al.* High TLR7 Expression Drives the Expansion of CD19(+)CD24(hi)CD38(hi) Transitional B Cells and Autoantibody Production in SLE Patients. *Frontiers in immunology* **10**, 1243 (2019).

30. Moir, S. *et al.* HIV-1 induces phenotypic and functional perturbations of B cells in chronically infected individuals. *Proceedings of the National Academy of Sciences* **98**, 10362-10367 (2001).

31. Luo, X. *et al.* Prognostic value of C-reactive protein in patients with COVID-19. *medRxiv*, 2020.2003.2021.20040360 (2020).

32. Ma, J. *et al.* Potential effect of blood purification therapy in reducing cytokine storm as a late complication of critically ill COVID-19. *Clinical immunology (Orlando, Fla.)* **214**, 108408 (2020).

33. Dang, V.D., Hilgenberg, E., Ries, S., Shen, P. & Fillatreau, S. From the regulatory functions of B cells to the identification of cytokine-producing plasma cell subsets. *Current opinion in immunology* **28**, 77-83 (2014).

34. Care, M.A. *et al.* Network Analysis Identifies Proinflammatory Plasma Cell Polarization for Secretion of ISG15 in Human Autoimmunity. *Journal of immunology (Baltimore, Md. : 1950)* **197**, 1447-1459 (2016).

35. Jego, G. *et al.* Plasmacytoid dendritic cells induce plasma cell differentiation through type I interferon and interleukin 6. *Immunity* **19**, 225-234 (2003).

36. Rosser, E.C. & Mauri, C. Regulatory B cells: origin, phenotype, and function. *Immunity* **42**, 607-612 (2015).

Figure Legends

Figure 1 – Critically ill SARS-CoV-2 patients display robust antibody secreting cell responses

(a-f) Peripheral blood mononuclear cells (PBMCs) were isolated from healthy donors, or PCR+ SARS-CoV-2 patient bloods. Isolated cells were stained and analyzed by flow cytometry. (a) CD19+ B cell fraction of total CD45+ cells. (b) Gating strategy for the identification of primary and secondary B cell populations. (c) Heatmap of secondary population frequency z-scores by healthy donor (grey) and SARS-CoV-2+ (green) patients. Associated dendrograms are representative of hierarchical clustering of both patient samples and B cell populations by Ward's method. (d) Representative plots, and statistical analysis of ASC frequencies of CD19+ B cells in SARS-CoV-2+ patients, vs healthy donors. (e) Representative plots, and statistical analysis of CD138+ ASC (ASC3) frequencies of total ASCs in SARS-CoV-2+ patients, vs healthy donors. (f) ASC frequencies of CD19+ B cells colored by patient gross disease severity (grey - healthy donor/asymptomatic; blue - outpatient/mild disease; green - ICU admitted/critically ill; red - deceased). (a, d-e) Student's t testing displayed between groups. (f) ANOVA analysis with Tukey's multiple comparison testing between groups. (a-f) *p <= 0.05; **p <= 0.01; ***p <= 0.001; **** p <= 0.0001.

Figure 2 – COVID-19 disease activity is highly associated with extrafollicular pathway activation

(a-j) Peripheral blood mononuclear cells (PBMCs) were isolated from healthy donor (HD), SARS-CoV-2 PCR+, vaccinated, or systemic lupus erythematosus (SLE) patient bloods. Isolated cells were stained and analyzed by flow cytometry. (a) Heatmap of secondary population frequency z-scores by outpatient (blue), ICU admitted (green), or deceased (red) SARS-CoV-2+ patients. Kidney failure identified and displayed as presence (orange) or absence (purple) of serious renal involvement as assessed by patient clinic notes. Associated dendrograms represent hierarchical clustering of both patient samples and B cell populations by Ward's method. Two major patient clusters are identified and designated extrafollicular-COVID (EF-Cov), or transitional COVID (Tr-Cov). (b) Patient sample collection times following symptom onset in EF-Cov and Tr-Cov clusters. (c) ASC frequency of CD19+ B cells in HD, EF-Cov, Tr-Cov, or vaccinated patients. Flu Vax -

seasonal influenza vaccinated; Hep A - hepatitis A vaccinated; Tetanus - tetanus toxoid vaccinated; YFV - yellow fever vaccinated. (d) CD138+ ASC frequency of ASCs in HD, EF-Cov, or Tr-Cov patients. (e) aN frequency of CD19+ B cells in HD, EF-Cov, or Tr-Cov patients. (f) DN2 frequency of CD19+ B cells in HD, EF-Cov, or Tr-Cov patients. (g) Representative flow plots displaying DN population composition in HD, EF-Cov, Tr-Cov, and SLE patient groups. (h-i) DN composition analysis in HD, EF-Cov, Tr-Cov, and SLE patient groups. (h) Mean DN population composition. (j-k) Chemokine receptor surface expression in follicular (rN, DN1) vs. extrafollicular (aN, DN2) populations observed in EF-Cov patients. (l-m) Multiplex assessment of cytokine concentrations in HD, EF-Cov, or Tr-Cov cluster patient samples. (b) Student's t testing displayed between groups. (c-f, h, j-m) ANOVA analysis with Tukey's multiple comparison testing between groups. (a-l) *p <= 0.05; **p <= 0.01; ***p <= 0.001; **** p <= 0.0001.

Figure 3 - Transitional B cell loss is associated with Ef response activation

(a-k) Peripheral blood mononuclear cells (PBMCs) were isolated from healthy donor (HD), SARS-CoV-2 PCR+, vaccinated, or systemic lupus erythematosus (SLE) patient bloods. Isolated cells were stained and analyzed by flow cytometry. (a) Transitional B cell frequency of CD19+ B cells in HD, EF-Cov, or Tr-Cov patients. (b) Representative flow plots displaying transitional population frequency in HD, and Tr-Cov patient groups. (c) $CD21^{lo}$ Transitional B cell frequency of CD19+ B cells in HD, EF-Cov, or Tr-Cov patients. (d) Representative flow plots displaying transitional population composition in HD, EF-Cov, and Tr-Cov patient groups. (e-h) Surface-expression phenotypes of $CD21^{lo}$ Transitional B cells from a SARS-CoV-2 patient (red), in comparison to total transitional B cells (green), or resting naive B cells (grey) from a healthy donor. (i) Representative flow plot displaying transitional population frequency in an SLE patient. (j) Representative flow plots displaying transitional population frequency in patients at d0, d12, and d20 following yellow fever vaccination. (k) Time course of transitional population frequency following yellow fever vaccination. (a, c) ANOVA analysis with Tukey's multiple comparison testing between groups. *p <= 0.05; **p <= 0.01; ***p <= 0.001; **** p <= 0.0001.

Figure 4 - EF pathway activation predicts poor disease outcomes

(a) Timeline of relevant medical events for four (4) longitudinally tracked ICU patients in the EF-Cov [EF-1, EF-2] and Tr-Cov [Tr-1, Tr-2] clusters. (b) Transitional B cell frequency of CD19+ B cells in patients from [a] over three collection time points. (c) Transitional B cell frequency of CD19+ B cells in patients from [a] over three collection time points. (d) Sequential Organ Failure Assessment (SOFA) scores of patients from [a] over three collection time points. (e) PaO2/FiO2 ratios of patients from [a] over three collection time points. (f) CRP values assessed by singleplex immunoassay for patients from [a] across three collection time points. (g) CRP values assessed by singleplex immunoassay from blood plasma collected from HD, EF-Cov, or Tr-Cov patients. (h) Linear regression of log(CRP) values as a function of transitional B cell frequency of CD19+ B cells. (i) Linear regression of log(CRP) values as a function of DN2 B cell frequency of total DN B cells. (i) Linear regression of CRP values as a function of IL-6 plasma levels. (g) ANOVA analysis with Tukey's multiple comparisons testing between groups. *p <= 0.05; **p <= 0.01; ***p <= 0.001; **** p <= 0.0001.

Figure 1

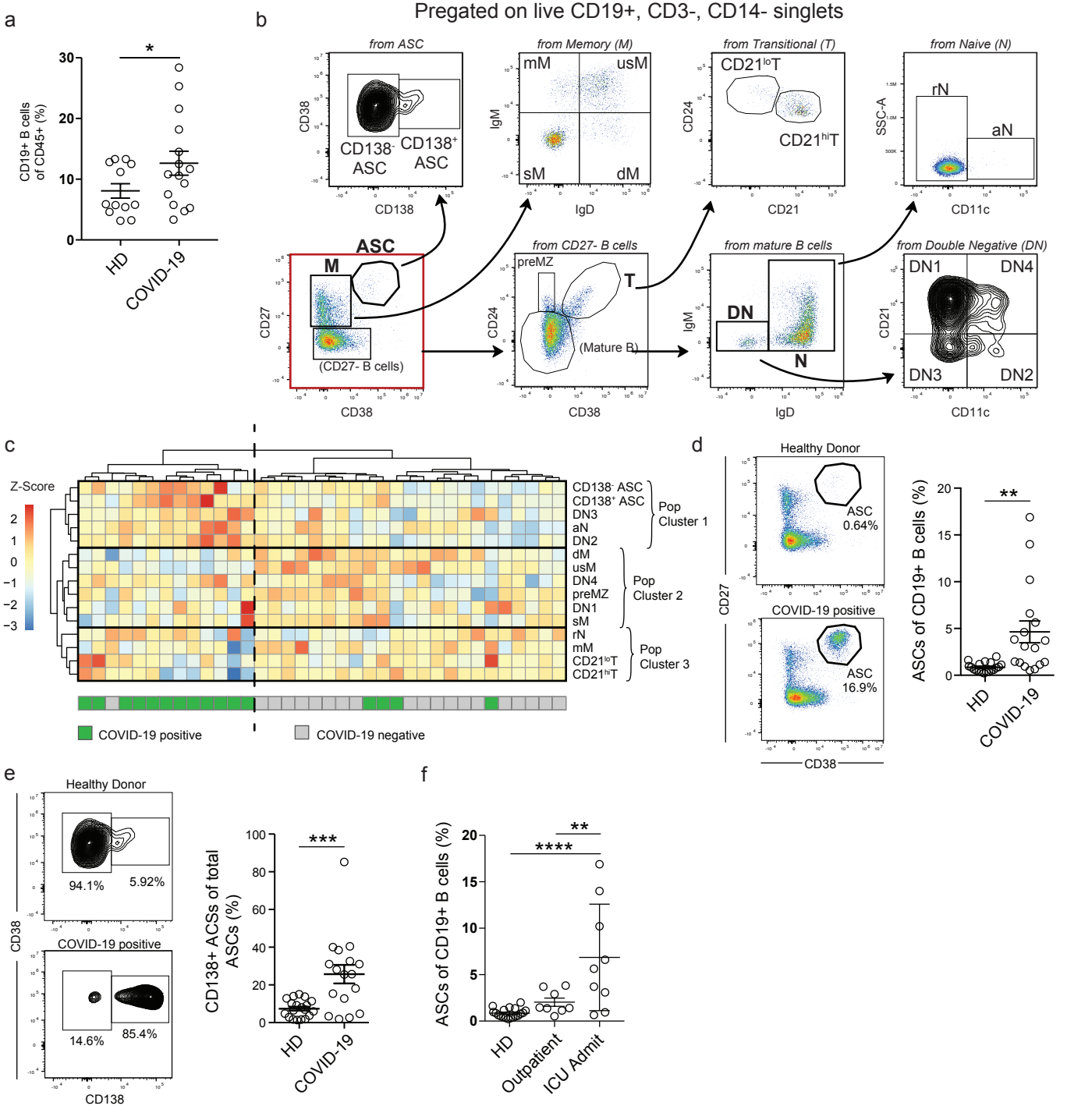
a
CD19+ B cells of CD45+ (%)
HD
COVID-19
b
Pregated on live CD19+, CD3-, CD14- singlets
from ASC
CD138- ASC
CD138+ ASC
CD38
CD138
from Memory (M)
mM
usM
sM
dM
IgM
IgD
from Transitional (T)
CD21loT
CD21hiT
CD24
CD21
from Naive (N)
rN
aN
SSC-A
CD11c
ASC
M
(CD27- B cells)
CD27
from CD27- B cells
preMZ
T
(Mature B)
from mature B cells
DN
N
from Double Negative (DN)
DN1
DN4
DN3
DN2
c
Z-Score
CD138- ASC
CD138+ ASC
DN3
aN
DN2
dM
usM
DN4
preMZ
DN1
sM
rN
mM
CD21loT
CD21hiT
Pop Cluster 1
Pop Cluster 2
Pop Cluster 3
COVID-19 positive
COVID-19 negative
d
Healthy Donor
ASC 0.64%
COVID-19 positive
ASC 16.9%
CD27
CD38
ASCs of CD19+ B cells (%)
HD
COVID-19
e
Healthy Donor
94.1%
5.92%
COVID-19 positive
14.6%
85.4%
CD38
CD138
CD138+ ACSs of total ASCs (%)
HD
COVID-19
f
ASCs of CD19+ B cells (%)
HD
Outpatient
ICU Admit

Figure 2

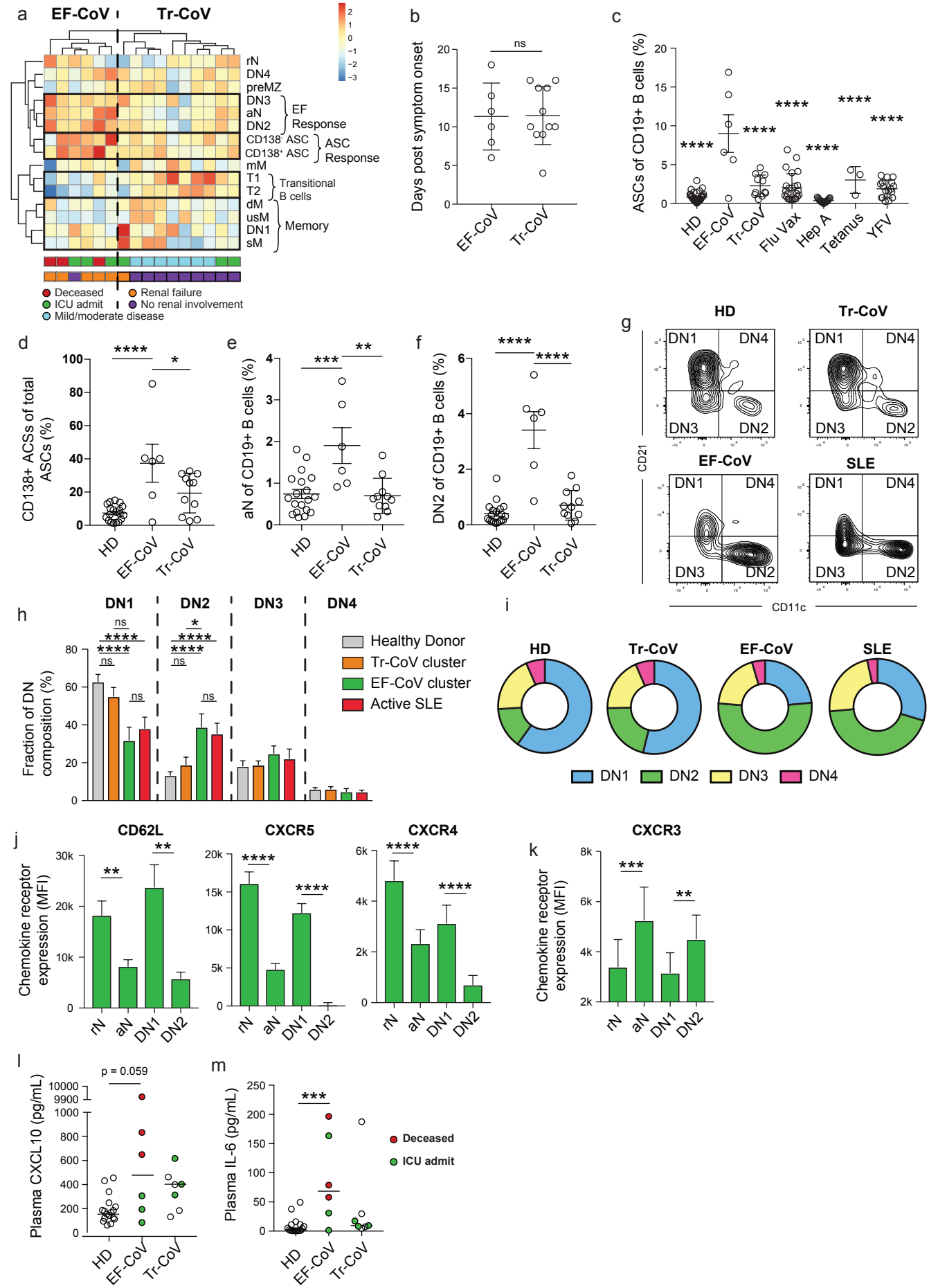
a
EF-CoV
Tr-CoV
Z-Score
rN
DN4
preMZ
DN3
aN
DN2
EF Response
CD138- ASC
CD138+ ASC
ASC Response
mM
T1
T2
Transitional B cells
dM
usM
DN1
sM
Memory
Deceased
ICU admit
Mild/moderate disease
Renal failure
No renal involvement
b
Days post symptom onset
ns
EF-CoV
Tr-CoV
c
ASCs of CD19+ B cells (%)
HD
EF-CoV
Tr-CoV
Flu Vax
Hep A
Tetanus
YFV
d
CD138+ ACSs of total ASCs (%)
e
aN of CD19+ B cells (%)
f
DN2 of CD19+ B cells (%)
g
HD
Tr-CoV
EF-CoV
SLE
DN1
DN4
DN3
DN2
CD21
CD11c
h
DN1
DN2
DN3
DN4
Fraction of DN composition (%)
Healthy Donor
Tr-CoV cluster
EF-CoV cluster
Active SLE
i
HD
Tr-CoV
EF-CoV
SLE
DN1
DN2
DN3
DN4
j
CD62L
CXCR5
CXCR4
Chemokine receptor expression (MFI)
rN
aN
DN1
DN2
k
CXCR3
l
Plasma CXCL10 (pg/mL)
p = 0.059
m
Plasma IL-6 (pg/mL)
Deceased
ICU admit

Figure 3

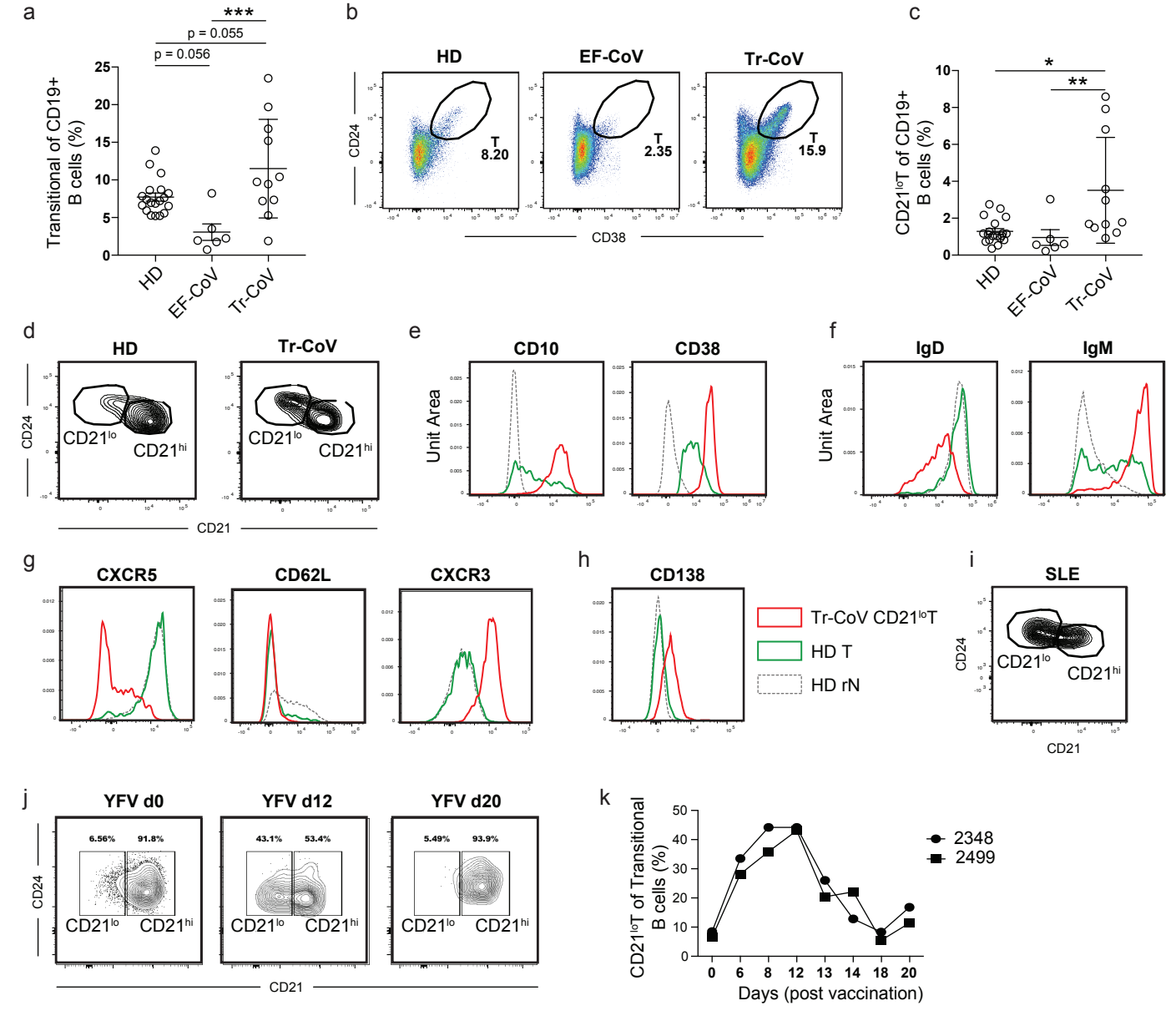
a
***
p = 0.055
p = 0.056
Transitional of CD19+ B cells (%)
HD
EF-CoV
Tr-CoV
b
HD
EF-CoV
Tr-CoV
CD24
CD38
T 8.20
T 2.35
T 15.9
c
*
**
CD21loT of CD19+ B cells (%)
HD
EF-CoV
Tr-CoV
d
HD
Tr-CoV
CD24
CD21
CD21lo
CD21hi
e
CD10
CD38
Unit Area
f
IgD
IgM
Unit Area
g
CXCR5
CD62L
CXCR3
h
CD138
Tr-CoV CD21loT
HD T
HD rN
i
SLE
CD24
CD21
CD21lo
CD21hi
j
YFV d0
YFV d12
YFV d20
6.56%
91.8%
43.1%
53.4%
5.49%
93.9%
CD24
CD21
CD21lo
CD21hi
k
CD21loT of Transitional B cells (%)
Days (post vaccination)
2348
2499

Figure 4

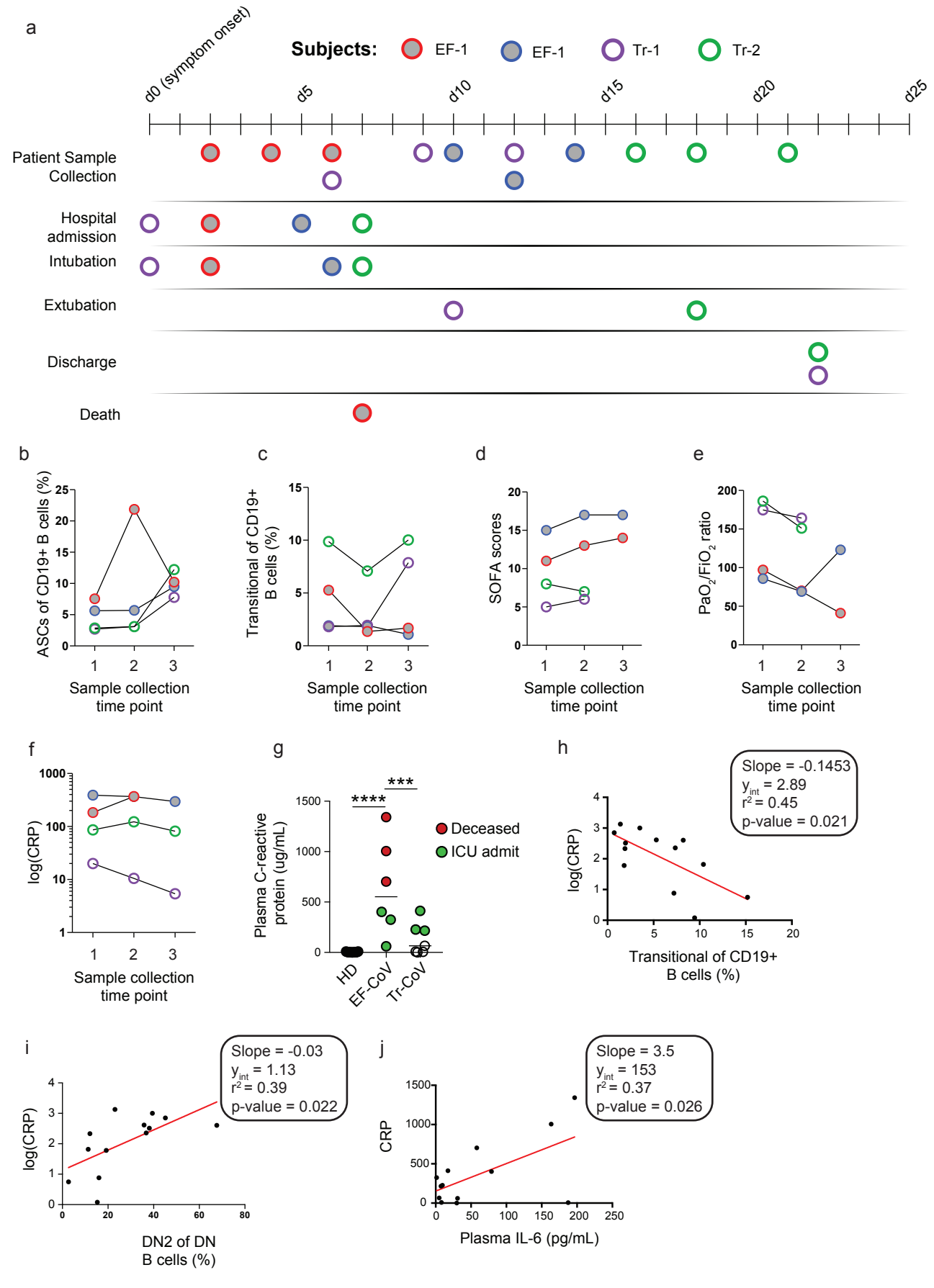
a
Subjects:
EF-1
EF-1
Tr-1
Tr-2
d0 (symptom onset)
d5
d10
d15
d20
d25
Patient Sample Collection
Hospital admission
Intubation
Extubation
Discharge
Death
b
ASCs of CD19+ B cells (%)
Sample collection time point
c
Transitional of CD19+ B cells (%)
Sample collection time point
d
SOFA scores
Sample collection time point
e
PaO2/FiO2 ratio
Sample collection time point
f
log(CRP)
Sample collection time point
g
Plasma C-reactive protein (ug/mL)
****
***
Deceased
ICU admit
HD
EF-CoV
Tr-CoV
h
Slope = -0.1453
yint = 2.89
r2 = 0.45
p-value = 0.021
log(CRP)
Transitional of CD19+ B cells (%)
i
Slope = -0.03
yint = 1.13
r2 = 0.39
p-value = 0.022
log(CRP)
DN2 of DN B cells (%)
j
Slope = 3.5
yint = 153
r2 = 0.37
p-value = 0.026
CRP
Plasma IL-6 (pg/mL)

Supplemental table 1

B-cell Core	B-cell Ext.	Activation	Homing
Live/Dead	CD1c	CD40	CD62L
CD3/CD14	CD10	CD69	CXCR3
CD19	CD11c	CD86	CXCR4
CD45	CD21	HLA-DR	CXCR5
IgD	CD24	PD-1	
IgM	CD27		
IgG	CD38		
	CD138		

Table 1 - Spectral Flow B cell Panel Design
Standardized panel design for the broad characterization and study of peripheral blood B cells

Supplemental table 2

Characteristic	All Subjects (n = 39)		
	Healthy Controls (n = 22)	Non-Critically-Ill COVID-19-Positive Subjects (n = 8)	Critically-Ill COVID-19-Positive Subjects (n = 9)
Mean age (range) – yr*	35±11 (22-61)	34±5 (26-44)	61±13 (34-81)
Gender – no. (%)			
Male	8 (36)	6 (75)	5 (56)
Female	14 (64)	2 (25)	4 (44)
Race – no. (%)			
Caucasian	14 (64)	6 (75)	1 (11)
African-American	0 (0)	0 (0)	7 (78)
Asian	7 (32)	2 (25)	1 (11)
Other	1 (5)		
Smoking History – no. (%)			
Never smoked	20 (91)	7 (88)	8 (89)
Former smoker	2 (9)	1 (13)	1 (11)
Current smoker	0 (0)	0 (0)	0 (0)
Symptoms – no. (%)			
Any	0 (0)	8 (100)	9 (100)
Fever	0 (0)	4 (50)	7 (78)
Conjunctival congestion	0 (0)	0 (0)	0 (0)
Nasal congestion	0 (0)	5 (63)	0 (0)
Anosmia	0 (0)	2 (25)	(0)
Headache	0 (0)	4 (50)	3 (33)
Cough	0 (0)	6 (75)	8 (89)
Sore Throat	0 (0)	4 (50)	1 (11)
Shortness of breath	0 (0)	1 (13)	7 (78)
Nausea or vomiting	0 (0)	0 (0)	0 (0)
Diarrhea	0 (0)	1 (13)	2 (22)
Myalgia or arthralgia	0 (0)	4 (50)	3 (33)
Chills	0 (0)	4 (50)	4 (44)
History – days			
Mean interval (range) between symptom onset and presentation***		1.7±0.8 (1-3)	3.9±2.3 (0-7)
Mean interval (range) between presentation and intubation			1.1±1.3 (0-3)
Mean interval (range) between symptom onset and sample collection		10.3±4.3 (4-16)	12.1±5.7 (2-22)
Comorbidities – no. (%)			
COPD	0 (0)	0 (0)	2 (22)
Diabetes	2 (9)	0 (0)	4 (44)
Hypertension	3 (14)	0 (0)	7 (77)
Coronary artery disease	0 (0)	0 (0)	2 (22)
Cerebrovascular disease	0 (0)	0 (0)	0 (0)
Cancer	0 (0)	0 (0)	0 (0)
Chronic Kidney Disease	0 (0)	0 (0)	2 (22)
Liver Disease	0 (0)	0 (0)	0 (0)
Immunodeficiency	0 (0)	0 (0)	0 (0)
Vital signs at presentation – no. (%)			
Mean arterial pressure			85±21
Respiratory rate			22±6
Heart rate			84±12
Temperature			37.1±0.3
Fever – no. (%)			
Fever on admission			0 (0)
Fever during hospitalization			8 (89)

Supplemental table 2 (cont'd)

Tmax during hospitalization – °C			38.8±0.9
Diagnosis of SARS-COV-2			
PCR amplification of nasopharyngeal swab		7 (88%)	9 (100)
Serum anti-SARS-COV-2		1 (13%)	0 (0)
Laboratory Findings – no. (%)			
White blood cell count			13.1±5.4
Absolute lymphocyte count[$]			1.24±0.5
Absolute neutrophil count[$]			9.11±4.5
Hemoglobin			9.7±1.8
Platelet count			273±105
Creatinine			3.7±3.4
Aspartate aminotransferase			68±63
Alanine aminotransferase			48±47
Total bilirubin			1.1±1.4
C-reactive protein[%]			190±130
Lactate dehydrogenase[#]			388±183
Creatine kinase[$]			261±347
Troponin I[%]			0.23±0.4
D-dimer			9097±12961
Radiographic Findings – no. (%)			
Interstitial abnormalities			9 (100)
Mediastinal lymphadenopathy			0 (0)
Consolidative opacities			2 (22)
Measures of Illness Severity			
PaO_2/FiO_2 Ratio[&]			141±68
SOFA Score**[&]			10.7±4.6
Complications – no. (%)			
Shock		0 (0)	8 (89)
Acute respiratory distress syndrome		0 (0)	9 (100)
Acute kidney Injury		0 (0)	6 (67)
Cardiomyopathy		0 (0)	0 (0)
Hemophagocytic lymphohistiocytosis		0 (0)	0 (0)
Treatments – no. (%)			
Antibacterial antibiotics		0 (0)	8 (89)
Antiviral antibiotics		0 (0)	4 (44)
Antifungal antibiotics		0 (0)	0 (0)
Systemic glucocorticoids		0 (0)	0 (0)
Hydroxychloroquine		0 (0)	6 (67)
Azithromycin		0 (0)	4 (44)
Mechanical ventilation		0 (0)	9 (100)
Vasopressors		0 (0)	8 (89)
Extracorporeal membrane oxygenation		0 (0)	1 (11)
Renal-replacement therapy		0 (0)	2 (22)
Intravenous immune globulin		0 (0)	0 (0)
Outcomes – no. (%)			
Admission to hospital		0 (0)	9 (100)
Discharge from hospital		0 (0)	2 (22)
Death		0 (0)	3 (33)
Recovery		8 (100)	4 (44)
Ongoing critical illness		0 (0)	2 (22)

Table 2. Baseline Demographic Characteristics of Research Subjects*

* Plus-minus values are means±SD. Percentages may not total 100 because of rounding.

Supplemental table 2 (cont'd)

** SOFA stands for Sequential Organ Failure Assessment
*** Data for time between symptom onset and presentation to clinical site were missing for one subject
$ Data for absolute lymphocyte count, absolute neutrophil count, and creatine kinase were missing or partially missing for four subjects
% Data for CRP and troponin I were missing or partially missing from two subjects
# Data for lactate dehydrogenase were missing or partially missing from three subjects
& Data for PaO_2/FiO_2 ratio were missing for three subjects upon extubation, therefore SOFA scores could not be calculated and therefore this average is higher than if these values were included

Supplemental table 3

Transitional B cells

Primary population

T: CD19^{pos} CD27^{neg} CD38^{int} CD24^{pos}

Secondary populations

CD21^{lo}T: CD24^{hi} CD21^{neg}

CD21^{hi}T: CD24^{lo} CD21^{pos}

Naive B cells

Primary population

N: CD19^{pos} CD27^{neg} CD38^{neg} CD24^{neg} IgD^{+}

Secondary populations

aN: CD11c^{pos}

rN: CD11c^{neg}

Double Negative B cells

Primary population

DN: CD19^{+} CD27^{neg} CD38^{neg} CD24^{neg} IgD^{neg}

Secondary populations

DN1: CD11c^{neg} CD21^{pos}

DN2: CD11c^{pos} CD21^{neg}

DN3: CD11c^{neg} CD21^{neg}

DN4: CD11c^{pos} CD21^{pos}

Memory B cells

Primary population

M: CD19^{pos} CD27^{pos} CD38$^{neg\text{-}lo}$

Secondary populations

mM: IgM^{pos} IgD^{neg}

dM: IgM^{neg} IgD^{pos}

usM: IgM^{pos} IgD^{pos}

sM: IgM^{neg} IgD^{neg}

Ab secreting cells

Primary population

ASC: CD19^{pos} CD27^{pos} CD38^{hi}

Secondary populations

CD138^{neg} ASC: CD138^{neg}

CD138^{pos} ASC: CD138^{pos}

Table 3 – Standard B cell definitions
Surface staining definintions of primary and secondary populations used for multivariate clustering and analysis.